JARO 7: 317–328 (2006)
DOI: 10.1007/s10162-006-0046-7

JARO
Journal of the Association for Research in Otolaryngology

Age-Related Changes in Cochlear Gene Expression In Normal and Shaker 2 Mice

Tzy-Wen L. Gong,[1] I. Jill Karolyi,[2] James MacDonald,[3] Lisa Beyer,[1] Yehoash Raphael,[1] David C. Kohrman,[1,2] Sally A. Camper,[2] and Margaret I. Lomax[1]

[1]*Kresge Hearing Research Institute, Department of Otolaryngology/Head–Neck Surgery, University of Michigan Medical School, Ann Arbor, MI 48109-0648, USA*
[2]*Department of Human Genetics, University of Michigan Medical School, Ann Arbor, MI 48109, USA*
[3]*University of Michigan Cancer Center, University of Michigan Medical School, Ann Arbor, MI 48109, USA*

Received: 5 August 2005; Accepted: 19 May 2006; Online publication: 23 June 2006

ABSTRACT

The vertebrate cochlea is a complex organ optimized for sound transduction. Auditory hair cells, with their precisely arranged stereocilia bundles, transduce sound waves to electrical signals that are transmitted to the brain. Mutations in the unconventional myosin XV cause deafness in both human *DFNB3* families and in shaker 2 (*sh2*) mice as a result of defects in stereocilia. In these mutant mice, hair cells have relatively normal spatial organization of stereocilia bundles but lack the graded, stair-step organization. We used *sh2* mice as an experimental model to investigate the molecular consequences of the *sh2* mutation in the *Myo15* gene. Gene expression profiling with Affymetrix GeneChips in deaf homozygous (*sh2/sh2*) mice at 3 weeks and 3 months of age, and in age-matched, normal-hearing heterozygotes (*+/sh2*) identified only a few genes whose expression was affected by genotype, but a large number with age-associated changes in expression in both normal mice and *sh2/sh2* homozygotes. Microarray data analyzed using Robust Multiarray Average identified *Aim1*, *Dbi*, and *Tm4sf3* as genes with increased expression in *sh2/sh2* homozygotes. These increases were confirmed by quantitative reverse transcription-polymerase chain reaction. Genes exhibiting altered expression with age encoded collagens and proteins involved in collagen maturation, extracellular matrix, and bone mineralization. These results identified potential cellular pathways associated with myosin XV defects, and age-associated molecular events that are likely to be involved in maturation of the cochlea and auditory function.

Keywords: myosin XV, gene expression profiling, collagen, bone

Abbreviations: RMA – Robust Multiarray Average; RT-qPCR – reverse transcriptase-quantitative polymerase chain reaction

INTRODUCTION

Mouse deafness mutants have provided significant insights into the genetic basis of hereditary deafness, ready access to cochlear pathology resulting from the mutant protein, and insights into the regulatory circuits required for normal cochlear development, homeostasis, and function. The extensively studied shaker 2 (*sh2*) mouse mutant (Deol 1954, 1955) has defects in stereocilia maturation, leading to profound deafness as a result of a missense mutation in the motor domain of myosin XV (Probst et al. 1998). This point mutation causes an amino acid change of cysteine to tyrosine. A second allele, $sh2^J$, harbors a deletion of a predicted C-terminal FERM domain of the myosin XV tail, which has been suggested to interact with cytoplasmic domains of integral membrane proteins (Anderson et al. 2000). Homozygous *sh2* and $sh2^J$ mice have identical cochlear pathology, i.e., abnormally short stereocilia at the apical surface of cochlear and vestibular hair cells, and abnormal actin filament-rich structures ("cytocauds") that orig-

Correspondence to: Margaret I. Lomax · Kresge Hearing Research Institute, Department of Otolaryngology/Head–Neck Surgery · University of Michigan Medical School · 9301E Medical Sciences Research Building III, Box 0648, Ann Arbor, MI 48109-0648, USA. Telephone: +1-734647-0952; fax: +1-734615-8111; email: mlomax@umich.edu

inate at the cuticular plate and project out from the basal end of the hair cell (Probst et al. 1998; Anderson et al. 2000; Beyer et al. 2000). Stereocilia lack the graded, stair-step organization, in spite of the normal spatial organization of stereocilia bundles (Anniko et al. 1980; Belyantseva et al. 2003). Mutations in human *MYO15A* also cause congenital, profound deafness in several *DFNB3* families (Wang et al. 1998; Friedman et al. 2002). Despite the identification of *MYO15A* as the defective gene, we do not understand at the molecular level how defective myosin XV proteins lead to stereocilia malformation or to subsequent long-term effects on cochlear pathology in affected members of *DFNB3* families or in *sh2* mice.

Unconventional myosins bind various cellular constituents via their divergent C-terminal "tail" domains and transport these cargos along polymerized actin filaments (Mermall et al. 1998). Myosin XV is normally located at the tips of stereocilia and within the actin-rich cuticular plate that anchors the bases of the stereocilia (Liang et al. 1999; Belyantseva et al. 2003). Myosin XV was recently shown to be essential in transporting whirlin to the tips of stereocilia (Belyantseva et al. 2005; Delprat et al. 2005; Kikkawa et al. 2005). Defective myosin XV proteins in *sh2* mice disrupt relevant structural interactions and/or biochemical pathways associated with this transport system and lead to stereocilia malformation.

Myosin XV may provide additional functions in sensory hair cells, such as in the active process of actin polymerization, leading to consequences beyond those immediately apparent changes in cytoskeletal architecture and to functional changes through alterations in gene expression. Small guanosine triphosphate (GTP) binding proteins such as Rho, known to regulate actin polymerization events, are also known to regulate gene transcription (Hall 1998). Activation of serum response factor, a key transcription factor, depends on appropriate control of actin polymerization (Sotiropoulos et al. 1999). We hypothesized that the *Myo15* mutation in *sh2* mice directly or indirectly affects homeostatic mechanisms, leading to changes in the steady-state transcript levels of genes that operate in compensatory pathways. To identify these pathways, we used Affymetrix GeneChips to profile gene expression in cochlear RNA from deaf *sh2/sh2* mice at 3 weeks and 3 months of age, and in normal-hearing heterozygotes (*+/sh2*) to control for age-related changes.

MATERIALS AND METHODS

Animals

Heterozygous *sh2* (*+/sh2*) females with normal auditory function were mated to *sh2/sh2* deaf males to generate *+/sh2* and *sh2/sh2* offspring. C57BL/6J mice were obtained from Jackson Laboratory (Bar Harbor, ME, USA). Mice of both genotypes were euthanized for cochlear RNA isolation at 3 weeks or 3 months of age. All animals were housed, cared for, and used in accordance with regulations of the University Committee on Use and Care of Animals (UCUCA).

Scanning electron microscopy

Morphological analysis of the inner ear was performed by scanning electron microscopy (SEM) and as described previously (Beyer et al. 2000). Three *+/sh2* and three *sh2/sh2* littermates were examined at 3 months of age. Briefly, mice were subjected to transcardiac perfusion using 2.5% glutaraldehyde in 0.15 M cacodylate buffer. The apex of the otic capsule was pierced to allow local perfusion through the round and oval windows. After an overnight fixation, cochleae were dissected further to reveal the surface of the organ of Corti and were stained with alternating osmium tetraoxide and thiocarbohydrazide, followed by dehydration in a graded series of ethanol and critical point drying with CO_2 in a SamDri 790 (Tousimis, Rockville, MD, USA). Surface morphology of the organ of Corti was viewed and photographed by SEM (Amray 1910 FE).

Cochlear dissection and RNA isolation

For microarray experiments, we pooled cochleae from 7 to 10 mice. Three independent pools were isolated from each of the four experimental groups (*+/sh2* at 3 weeks, *+/sh2* at 3 months, *sh2/sh2* at 3 weeks, and *sh2/sh2* at 3 months). Cochlear tissues, including the otic capsule but excluding vestibular tissues, were dissected either in phosphate-buffered saline or RNA*later* (Ambion, Austin, TX, USA), and RNA was isolated by using TRIzol (Invitrogen, Carlsbad, CA, USA). RNA subjected to reverse transcriptase-quantitative polymerase chain reaction (RT-qPCR) assays was first treated with RNase-free DNase I (10 units; Roche Applied Science, Indianapolis, IN, USA) at 37°C for 15 min, followed by purification on RNeasy spin columns (Qiagen, Valencia, CA, USA). RNA quality was assessed with Agilent Bioanalyzer 2100 (Agilent Technologies; New Castle, DE, USA); RNA concentration was determined by UV spectrophotometry. RNA yields averaged 0.5 μg per cochlea.

Microarray analysis

Cochlear gene expression was assessed with MG_U74Av2 GeneChip oligonucleotide arrays (Affymetrix, Santa Clara, CA, USA) on total cochlear RNA (3.5–5 μg) from three pools each of four experimental

groups. Synthesis of cRNA, hybridization to chips, and washes were performed in the University of Michigan Diabetes Research and Training Center (MDRTC) Microarray Core according to the Affymetrix protocol. GeneChips were processed in two separate batches. The first batch included one RNA sample for each of the four experimental groups; the second batch included two RNA samples for each group. GeneChips were scanned at 3-μm density with GeneArray Scanner (Affymetrix); images were inspected to ensure that all 12 chips had low background and bright hybridization signals.

Data analysis

Data analysis was performed at the University of Michigan Comprehensive Cancer Center Affymetrix and cDNA Microarray Core. We compared two different methods for data analysis: Robust Multiarray Average (RMA) analysis and quantile normalization of the trimmed means of the perfect match–mismatch (PM–MM) signals (differences between PM and MM values) (Giordano et al. 2001). In the former, expression values were calculated by using the RMA method, as implemented in the Bioconductor library of the R statistical language (http://www.bioconductor.org). RMA has been shown to give more reliable estimates of relative expression values when using "spike-in" samples that only differ for a known subset of probe sets. The same is true for a set of samples that were serially diluted before hybridization (Irizarry et al. 2003). We also demonstrate in this study that the RMA method is more reproducible, particularly for genes expressed at lower levels (details in Results and Fig. 2). Therefore, expression values derived from the RMA analysis were used in the following analyses. Expression values, $y_{ij(k)}$, were fitted to an ANOVA model on a gene-by-gene basis.

$$y_{ij(k)} = \alpha_{i(k)} + \beta_{j(k)} + (\alpha\beta)_{ij(k)} + \varepsilon_{ij(k)}$$

where α represents differences due to genotype (*sh2/sh2* vs. *+/sh2*); β indicates differences due to age (3 months vs. 3 weeks); $\alpha\beta$ accounts for differences due to a genotype × age interaction; ε is residual effects; and k indicates that each of these factors was nested in a batch effect, since the 12 samples were processed at two separate times. A nested model was used to account for obvious nonbiological differences between the batches. Data were analyzed with SAS Proc GLM, which uses sums of squares. Data were also analyzed using Proc Mixed, which fits a restricted maximum likelihood model. Both analyses yielded similar results.

Expression values from one GeneChip (*+/sh2* at 3 months) exhibited different density dynamics compared to the other 11 chips; therefore, this chip was excluded from subsequent analyses. Additional data analyses using dChip and a hierarchical clustering algorithm "Heat Map" (Eisen et al. 1998) indicated significant differences between the two batches of GeneChips: batch 1 (four chips) vs. batch 2 (eight chips), which were processed and hybridized at separate times to GeneChips of different lots. In other words, reproducibility was greatly improved when tissue samples were processed in parallel for RNA preparation and microarray hybridization using GeneChips of the same lot. Because the outlier chip came from the first batch, we also performed analyses with only the second batch of eight chips, i.e., two chips per group. Analyses derived from 11 chips and 8 chips were evaluated for consistent results. For each comparison (age × genotype interaction, genotype, and age main effects), p values were adjusted by using false discovery rate (FDR) (Storey 2002); significance was defined as $p < 0.01$. Fold changes between *+/sh2* and *sh2/sh2* or between 3-week- and 3-month-old mice were calculated to determine the direction and magnitude of changes.

Quantitative RT-PCR

Genotype-related changes in gene expression were confirmed by RT-qPCR assays on additional pools of RNA from 3-week-old *+/sh2* and *sh2/sh2* mice (4 pools for each genotype; 4–6 mice per pool), independent of those used in the GeneChip analysis. Age-related changes that were independent of the *Myo15* mutation were confirmed on cochlear RNA from C57BL/6J mice (4 mice per pool, 4 pools per age) at both ages. First strand cDNA was synthesized from total RNA (1 μg) with 200 units of RNase H⁻-MMLV reverse transcriptase (SuperScript III; Invitrogen) and oligo $(dT)_{12–18}$ (500 ng) in the presence of RNasin (20 units; Promega, Madison, WI, USA).

Real-time PCR was performed in a Prism 7000 Sequence Detection System (Applied Biosystems, Foster City, CA, USA) with TaqMan probes (Assays-on-Demand or Assays-by-Design; Applied Biosystems). For each gene assayed, triplicate cDNA samples derived from each RNA pool were assayed for quality control. To minimize experimental variability, multiple pools of RNA samples were simultaneously assayed, i.e., in the same PCR plate, for any given gene. As an internal control, we also determined the level of *S16* mRNA in each RNA sample. C_T, the threshold cycle, is defined as the PCR cycle number at which the fluorescence intensity is appreciably above the background level but is still in the early exponential phase of amplification. The difference in C_T between the gene of interest (gene "*X*") and *S16* for any given RNA sample was defined as $\Delta C_{T(X)}$. Individual $\Delta C_{T(X)}$

was adjusted to the averaged $\Delta C_{T(X)}$ of four replicates (derived from four independent pools of tissues) in the control group, i.e., 3 weeks in comparisons between two ages and *+/sh2* in comparisons between two genotypes. These adjusted values ($\Delta C_{T(X)adj}$) were subjected to statistical analysis by unpaired *t*-test (StatView; SAS Institute, Cary, NC, USA). The difference in $\Delta C_{T(X)adj}$ between two groups (e.g., 3 months vs. 3 weeks, *sh2/sh2* vs. *+/sh2*) was defined as $\Delta\Delta C_{T(X)adj}$, which represented a relative difference in expression of gene *X* (Livak and Schmittgen 2001). Fold difference was calculated as $2^{\Delta\Delta C_{T(X)adj}}$, assuming doubling of products every amplification cycle or 100% amplification efficiency.

RESULTS

Inner ear morphology

At 3 months, the organ of Corti of *+/sh2* mice had a normal appearance throughout most of the cochlea (Fig. 1A). Toward the basal hook region, we observed in two of the three mice examined occasional outer hair cell loss, while the inner hair cells remained intact (Fig. 1B). In *sh2/sh2* mutants, the surface morphology in the apex at 3 months closely resembled that observed at 3 weeks (Karolyi et al. 2003). Most outer and inner hair cells were present and could be identified by their stubby and poorly organized stereocilia on the apical surface (Fig. 1C). On the other

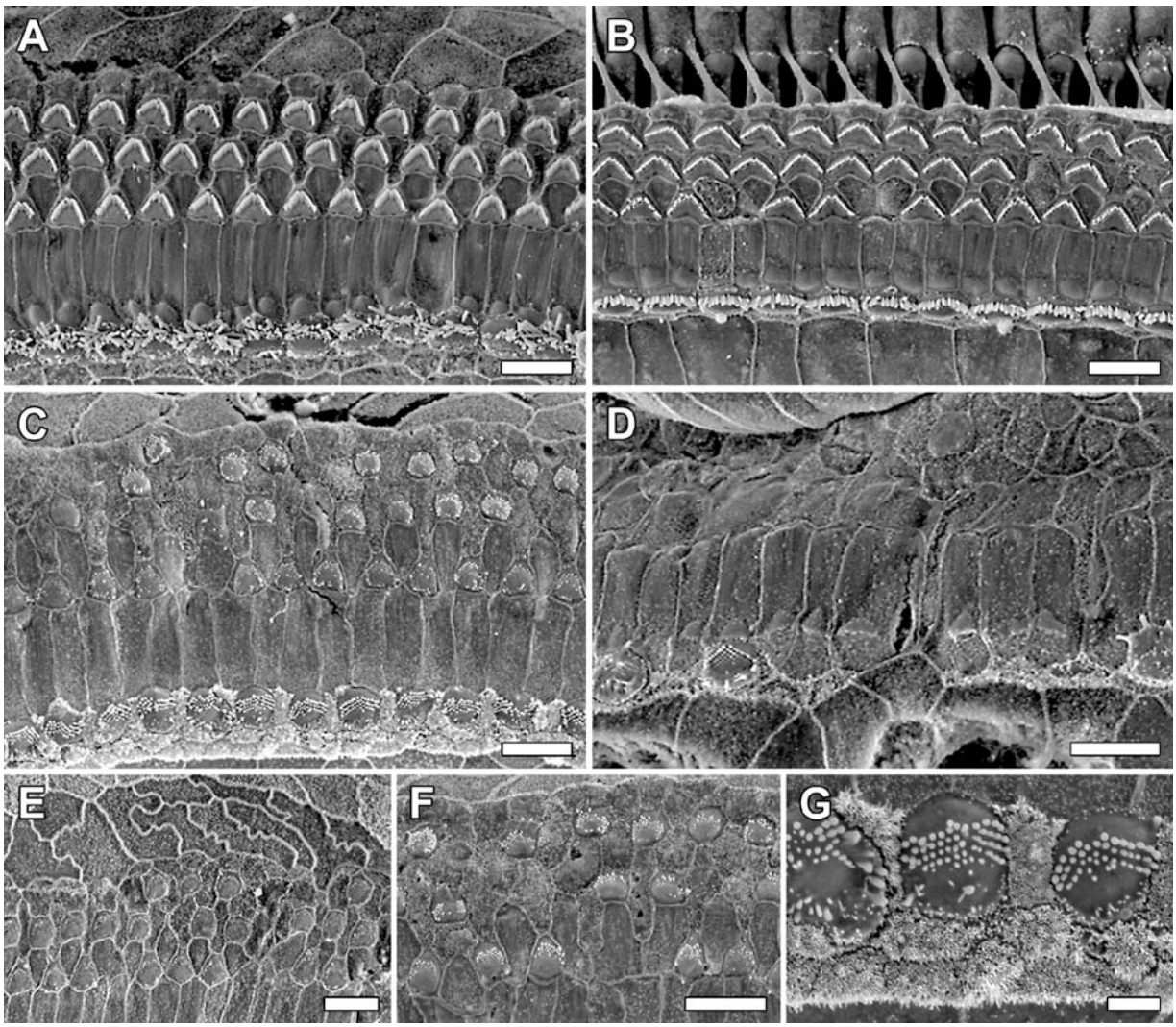

FIG. 1. Surface morphology of *+/sh2* and *sh2/sh2* cochleae at 3 months of age by SEM. (A, B) *+/sh2* mice. In *+/sh2* mice, the organ of Corti appeared normal in the apex (**A**). A few outer hair cells were missing in the basal hook region (**B**). (**C**–**G**) *sh2/sh2* mice. Most hair cells were present in the apex (**C**), but the apical diameter of outer hair cells appeared smaller than normal, and the supporting cells were expanded. In the basal hook region (**D**), there was considerable hair cell loss with most outer hair cells degenerated and few inner hair cells surviving. In the lower apex of the cochlear duct, Hensen cells had an irregular contour (**E**). Surviving outer and inner hair cells could be identified by short, disorganized stereocilia (**F** and **G**, respectively). The density of microvilli in inner phalangeal cells appeared to have increased (**G**), compared to normal cochleae (**B**).

hand, in the basal hook region most outer hair cells were no longer visible on the surface view (Fig. 1D). There is a gradual change in organ of Corti surface morphology along the cochlea. For example, in the lower apex and upper base regions, there was some loss of both inner and outer hair cells although most survived (Fig. 1E). Supporting cells appeared normal in general and expanded to fill spaces in areas of missing outer hair cells. Hensen cells had an irregular apical contour (Fig. 1E). Upon closer examination of the apical region, the outer hair cell surface was smaller in diameter and had extensive loss of stereocilia (Fig. 1F). On the inner hair cell surface, extra rows and ectopic location of stereocilia were commonly observed (Fig. 1G). Inner phalangeal cells had an excessive number of microvilli that were densely matted. Pillar cells survived throughout the length of the cochlea.

Dynamic range of gene expression in the mouse cochlea

We used Affymetrix mouse U74Av2 GeneChips to profile gene expression in mouse cochlear RNA and compared two different methods for data analysis. For genes with low expression values, expression values derived by RMA analysis were more reproducible (Fig. 2A) than data obtained by quantile normalization of the trimmed means of the PM–MM signals (Fig. 2B). Based on the average expression value for the 12 chips analyzed, all probe sets were ordered from the lowest (2.45) to the highest (14.42) value and grouped into four quartiles (Fig. 2C). The total number of probe sets in each quartile was counted to determine transcript frequencies. Table 1 presents the percentage of the 12,488 probe sets with expression values in each quartile. Genes expressed in limited cell types within the cochlea (Table 1) were distributed throughout this entire range. *Prph*, a marker of type II spiral ganglion neurons, was in the lowest quartile, consistent with type II neurons comprising only 5% of the spiral ganglion. *Myo6* and *Myo7a*, genes primarily expressed in hair cells in the cochlea, and supporting cell-specific genes *Hes5*, *Tecta*, and *Tectb* (α and β tectorins), were in the second quartile. Many genes with broader expression patterns, including *Pou3f4* (Brn4) in the otic capsule and *Gjb6* (Cx30) in the supporting cells and stria vascularis, were within the third quartile. Only 1.1% of the probe set had high expression values (the top quartile). *Gjb2* (Cx26) is widely distributed in the sensory epithelium, as are genes for the housekeeping proteins GAPDH, β-actin, and ribosomal proteins S16 and S18. Surprisingly, *Pou4f3* (Brn3.1), encoding a POU-domain transcription factor found exclusively in hair cells, was also highly expressed. Thus, although analysis of microarray data by previous methods based on PM–MM values failed to detect low abundance transcripts, RMA analysis of microarray data reproducibly detects genes with a wide

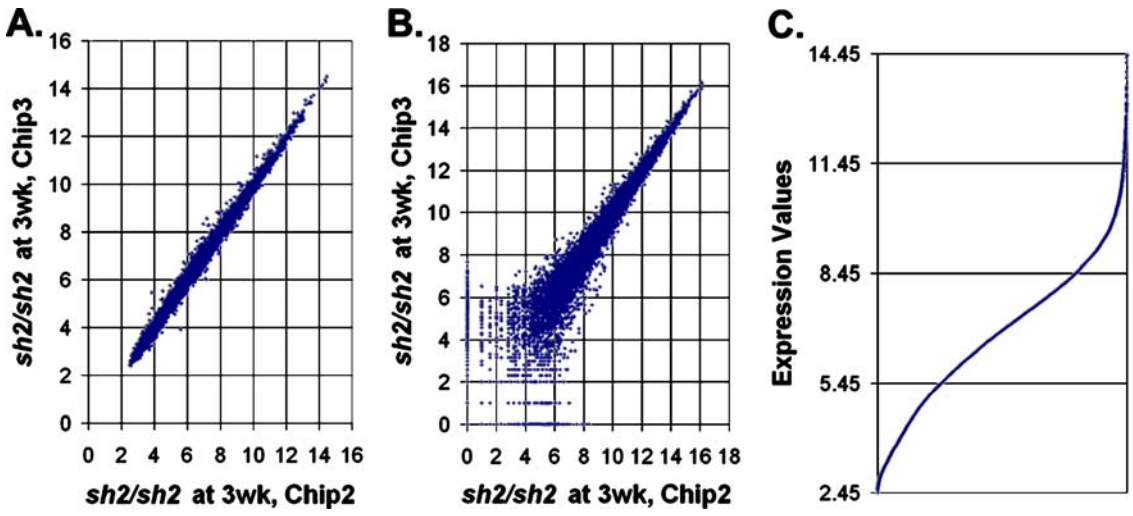

FIG. 2. Expression profiles of cochlear RNA from *+/sh2* and *sh2/sh2* mice. (**A**) Scatter plot of expression values derived from perfect match (PM) values only using RMA analysis. Expression profiles of two independent pools of cochlear RNA from the same experimental group, i.e., *sh2/sh2* at 3 weeks of age, were compared to each other. Note the high correlation between values, even at low signal intensities. (**B**) Scatter plot of signal intensity derived from geometric means of differences between PM and mismatch (MM) values. The same data extracted from Affymetrix GeneChips as in Figure 1A were processed by the geometric means of PM–MM values and transformed to log base 2. Note the poor signal-to-noise ratios at low signal intensities. (**C**) Dynamic range of gene expression values in the mouse cochlea. Averaged expression values, derived from PM signals of all 12,488 probe sets on all 11 mouse U74Av2 GeneChips and processed by RMA, were expressed to the log base 2 (*Y*-axis) and plotted (*X*-axis) from the lowest (2.45) at the left to the highest (14.42) at the right.

TABLE 1

Distribution of expression values of all 12,488 probe sets on MG_U74Av2 GeneChip oligonucleotide arrays

	Expression values	*Genes included*	
	Ranges	*Percentage (%)*	
1st quartile	2.45–5.44	26	*Gjb3, Gjb6, Myo1b, Pax6, Prph, Scn9a*
2nd quartile	5.45–8.43	54	*Atoh1, Myo7a, Hes5, Tecta, Tectb, Dia1, Col4a2*
3rd quartile	8.44–11.43	19	*Pou3f4, Gjb6, Otog*
4th quartile	11.44–14.42	1.1	*Gjb2, Pou4f3, Col1a1, β-actin, Gapdh, Actg1*

range of expression values, as well as those expressed in restricted cell types in the cochlea.

Differential gene expression in the *sh2/sh2* cochlea: genotype effects

To identify differentially expressed genes, we subjected each gene's expression values to two-way ANOVA. Two data sets were analyzed. Set 1 included data from all 11 GeneChips, excluding data from one GeneChip (3-month-old *+/sh2*) that exhibited different signal dynamics. Set 2 included only data from the eight RNA samples hybridized simultaneously to GeneChips (batch 2). Overall, 327 probe sets in data set 1, and 201 probe sets in data set 2, showed significant differences ($p < 0.01$; Fig. 3A) due to genotype (*sh2/sh2* vs. *+/sh2*), age (3 weeks vs. 3 months), or an age × genotype interaction. We conservatively focused on 123 probe sets identified in both data sets.

Only 11 genes (9%) showed expression significantly different in *sh2/sh2* vs. *+/sh2* mice (genotype effects) (Fig. 3B). Nine genes had modest increases (1.1- to 1.7-fold), whereas two genes had very small decreases (1.1- to 1.2-fold) in the *sh2/sh2* mice (Table 2). Based on their potential function and relevance in hair cells, we chose four genes for further analysis. These were *Tm4sf3*, *Aim1*, *Dbi*, and *Gas6*. TM4SF3, a small tetraspan membrane protein, interacts with other tetraspanins as well as a subset of β1 integrins (α3β1, α4β1, α6β1) (Serru et al. 1999). *Aim1* (absent in melanoma 1) encodes a nonlens member of the βγ-crystallin superfamily (Ray et al. 1997; Rajini et al. 2003) that may interact with the cytoskeleton, based on AIM1's homology to a member of the gelsolin superfamily of actin-binding proteins (Teichmann et al. 1998). *Dbi* (Diazepam binding inhibitor) encodes a small, 10-kDa protein that competes for the benzodiazepine binding site on type A GABA receptors in the brain and is thought to down-regulate GABA-mediated inhibitory responses (Costa and Guidotti 1991). *Gas6* (Growth arrest-specific gene 6) encodes a ligand for receptor tyrosine kinases Mer, Axl, or Sky to promote proliferation in several cell types (for review, see Melaragno et al. 1999; Yanagita 2004). Furthermore, Gas6 and its receptor Mer play a critical role in maintenance of vision function (Hall et al. 2002; Hall et al. 2003). Although we could not confirm the 20% decrease in *Gas6* mRNA in this whole cochlear preparation, we confirmed that *Tm4sf3*, *Aim1*, and *Dbi* had increased expression in *sh2/sh2* cochlear RNA. *Tm4sf3* mRNA was 1.7-fold higher in *sh2/sh2* cochlear RNA by microarray analysis and 2.2-fold higher ($p < 0.01$) by RT-qPCR. We observed a 1.2-fold increase for both *Aim1* and *Dbi* with microarrays, but greater increases (1.9- and 1.5-fold, respectively) by RT-qPCR (Table 2).

In comparison to the two-way ANOVA analysis with combined grouping, we also performed direct comparisons between the two genotypes at 3 weeks and at 3 months. Direct comparisons failed to identify the aforementioned genes, except for *Tacstd2* ($p < 0.05$). This result was not surprising, because combining the groups in two-way ANOVA gives a larger sample size (n) and is thus more powerful than comparing the individual groups with smaller sample numbers.

Age-related changes in genes for collagen and extracellular matrix proteins

A surprisingly large number of genes showed age-related changes in expression. Of the 123 probe sets,

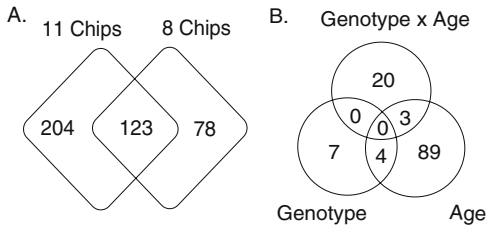

FIG. 3. Analysis of differentially expressed genes. (**A**) Comparison of different data sets. Two collections of differentially expressed probe sets were identified when we used expression values from all 11 chips (left diamond) vs. those from 8 chips (right diamond). There were 123 probe sets (overlap) common to both data sets. These 123 probe sets were analyzed further. (**B**) Venn diagrams of the number of probe sets with statistically significant differences ($p < 0.01$) due to age (96), genotype (11), or age × genotype effects (23). Some of the 123 probe sets showed significant differences in expression values between the two age groups or between the two genotypes, whereas others had different trends of age-related changes between the two genotypes (genotype × age interaction).

TABLE 2

Genes differentially expressed between *+/sh2* and *sh2/sh2* mice

Gene symbol	Gene name	Fold change[a]	
		Gene Chip[b]	RT-qPCR[c]
Aim1	Absent in melanoma 1	1.21	1.92
Bcl2a1d	B cell leukemia/lymphoma 2 related protein A1d[d]	1.19	
C4	Complement component 4, within H-2S[d]	1.48	
Dbi	Diazepam binding inhibitor[d]	1.24	1.50
Fbp2	Fructose bisphosphatase 2	1.21	
Rrad	Ras-related associated with diabetes; Rad, Rem3	1.12	
	RIKEN cDNA 1300007B12	1.11	
Tm4sf3	Transmembrane 4 superfamily member 3	1.72	2.23
Tacstd2	Tumor-associated calcium signal transducer 2[d]	1.54	
Gas6	Growth arrest specific 6	−1.20	NS
	RIKEN cDNA D330001F17Rik	−1.10	

[a]The ratio of the values in *sh2/sh2* to *+/sh2*. A negative number indicates a lower expression level in *sh2/sh2*.

[b]Changes calculated from averaged expression values derived by the RMA analysis as described in Materials and methods. Differences between two genotypes were statistically significant at $p < 0.01$.

[c]Changes were the average relative expression levels determined by RT-qPCR from four RNA pools each of 3-week-old *sh2/sh2* and *+/sh2* mice. Differences between two genotypes were statistically significant in all at $p < 0.01$. NS, statistically non-significant ($p > 0.05$).

[d]Also significantly different expression between 3 weeks and 3 months (age effect, $p < 0.01$).

96 (79%) had statistically significant ($p < 0.01$) differences in expression at 3 weeks vs. 3 months in both genotypes. Fifty-seven probe sets (corresponding to 44 genes) showed at least a 1.5-fold change (Table 3). Many genes with decreased expression at 3 months encoded collagen subunits or enzymes involved in collagen maturation. The mouse U74Av2 Chip contains probes for 28 collagen genes, whose expression values range from the lowest quartile (*Col3a1*, *Col4a3*, *Col7a1*, *Col14a*) to the highest (*Col1a1*) (Table 1). Expression of *Col13a1* showed only a moderate 1.5- to 1.7-fold decrease at 3 months, whereas *Col1a1*, *Col1a2*, *Col3a1*, *Col5a2*, *Col11a1*, and *Col11a2* consistently decreased at least 2-fold (Table 3). Also downregulated were genes for proteins involved in collagen cross-linking and maturation (*Lox*), in bone mineralization (*Akp2*, *Bglap1*) (Gopalakrishnan et al. 2001; Hessle et al. 2002), and in the extracellular matrix (ECM) (*Sparc*, *Npnt*). Most genes with higher expression at 3 months encoded cell antigens in either the histocompatibility or the immune response (Table 3). These increases in expression likely reflected changes in bone marrow maturation and blood cell infiltration in the apex of the otic capsule included in the dissected tissue.

We used real-time RT-PCR assays to confirm the age-related changes in a subset of genes, plus *Col15a1*, *Pou2af1*, and *Ifit1* on mouse cochlear RNA from C57BL/6J mice (Table 3). Of the 13 genes tested, 12 showed differential expression at these two ages at $p < 0.01$; the changes in *Pou2af1* were significant at $p < 0.05$ (Table 3). The magnitude of the changes determined by RT-qPCR was often greater than that determined by the microarray analysis.

Genes with age and genotype effects

In addition to differences in gene expression between *sh2/sh2* and *+/sh2* (the genotype effect), we were interested in differential responses over time between two genotypes associated with progressive deterioration in *sh2/sh2* mice, but not in *+/sh2*. These differential responses would be reflected in the genotype × age interaction term. Twenty-three probe sets had a genotype × age interaction term in two-way ANOVA ($p < 0.01$; Table 4), indicating that either the direction or extent of the change in expression differs with age in *+/sh2* vs. *sh2/sh2* mice. For 20 of those genes, there was no significant difference in expression due to either genotype or age alone. However, three of these genes, i.e., *P2rx4*, *Tcf3*, and *Sparc*, also showed genotype-independent age effects. *P2rx4*, a P2X purinergic receptor, was previously shown to be expressed in the rat organ of Corti and in both vestibular and cochlear spiral ganglion neurons (Xiang et al. 1999). In the microarray analysis, we observed a 55% increase in *P2rx4* expression with age in *+/sh2* heterozygotes, but only a 24% increase in *sh2/sh2* mice. *Tcf3* encodes a transcription factor implicated in Wnt/β-catenin signaling in early embryogenesis (Korinek et al. 1998). In this study, *Tcf3* showed a small but consistent decrease (14%) with age in *sh2/sh2* mice, but no age-related change in *+/sh2* mice. *Sparc*, one of the most abundant transcripts in both human fetal cochlear (Skvorak et al. 1999; Resendes et al. 2002) and mouse organ of Corti cDNA libraries (Beisel et al. 2004; Pompeia et al. 2004), encodes a Ca^{2+}-binding glycoprotein whose high-affinity binding to

TABLE 3

Genes with differential expression in the cochlea at 3 months vs. 3 weeks

Gene symbol	*Gene name*	*Fold change*[a] *GeneChip*[b]	*Fold change*[a] *RT-qPCR*[c]
Genes whose expression decreases with age			
	Expressed sequence tag AW047643	−1.50	
Acas2l	Acetyl CoA synthetase 2-like	−1.59	
Akp2	Alkaline phosphatase 2	−2.80	
Alas2	Aminolevulinic acid synthase 2, erythroid	−1.93	
Bglap1	Bone gamma carboxyglutamate protein 1	−3.02	
Calmbp1	Calmodulin binding protein 1	−1.63	
Ccnb2	Cyclin B2	−1.74	
Col1a1	Procollagen, type I, alpha 1	−3.91	−4.69
Col1a2	Procollagen, type I, alpha 2	−3.45	−3.46
Col3a1	Procollagen, type III, alpha 1	−2.35	
Col5a2	Procollagen, type V, alpha 2	−4.30	−4.06
Col11a1	Procollagen, type XI, alpha 1	−3.83	−6.02
Col11a2	Procollagen, type XI, alpha 2	−2.20	
Col13a1	Procollagen, type XIII, alpha 1	−1.51	−3.20
Col15a1	Procollagen, type XV, alpha 1	−1.71	−2.68
Gja1	Gap junction membrane channel protein alpha 1	−1.97	
Ibsp	Integrin binding sialoprotein	−2.81	
Kcnn4	K^+ intermediate/small conductance calcium-activated channel, subfamily N, member 4	−1.51	−1.88
Lifr	Leukemia inhibitory factor receptor	−1.83	
Lipc	Lipase, hepatic	−1.85	
Lox	Lysyl oxidase	−2.65	−2.28
Myo1b	Myosin 1B	−1.50	
Npnt	Nephronectin	−1.79	−4.20
Plp1	Proteolipid protein (myelin) 1	−1.65	
Pou2af1	POU domain, class 2,associating factor 1	−1.56	−1.49
Ppic	Peptidylprolyl isomerase C	−2.20	
Ptgis	Prostaglandin I2 (prostacyclin) synthase	−1.60	
Ptp4a3	Protein tyrosine phosphatase 4a3	−1.80	
Sparc	Secreted acidic cysteine rich glycoprotein; osteonectin[d]	−2.45	−3.46
Thbs1	Thrombospondin 1	−1.60	
Uhrf1	Ubiquitin-like, containing PHD and RING finger domains, 1	−1.57	
Vdr	Vitamin D receptor	−1.55	
Wisp1	Wnt1 inducible signaling pathway protein 1	−2.57	−3.86
Xpo7	Exportin 7; RAN binding protein 16	−1.72	
Genes whose expression increases with age			
	Expressed sequence tag AI893585	1.64	
Amy1	Amylase, salivary	1.69	
C4	Complement component 4[e]	1.71	
H2-Aa	Histocompatibility 2, class II antigen A, alpha	2.42	
H2-Ab1	Histocompatibility 2, class II antigen A, beta 1	1.61	
H2-Eb1	Histocompatibility 2, class II antigen E beta 1	1.64	
Ighg	Immunoglobulin heavy chain (gamma polypeptide)	7.36	
Igh-V7183	Immunoglobulin heavy chain V7183 family	9.25	
Igh-VJ558	Immunoglobulin heavy chain J558 family	11.22	
Igj	Immunoglobulin joining chain	4.50	
Igk-v21	Immunoglobulin kappa chain variable 21	3.55	
IgM	Immunoglobulin kappa light chain	2.10	
Ifit1	Interferon-induced protein with tetratricopeptide repeats 1	2.13	2.04

[a]Ratio of the values at 3 months vs. 3 weeks. A negative number indicates a decrease in expression with age.

[b]Change in average expression values in the *sh2* mice as described in Materials and methods. Differences between the two ages were greater than 1.5-fold and statistically significant ($p < 0.01$). Listed were genes common to both analysis of 11 and 8 chips, except *Col15a1*, *Pou2af1* (only in the analysis including 8 chips), and *Ifit1* (only in analysis including all 11 chips).

[c]Changes in cochlear mRNA levels in C57BL/6J mice (four pools each) determined by RT-qPCR. Differences between two ages were statistically significant in all at $p < 0.01$, except *Pou2af1* at $p < 0.05$.

[d]Also exhibited an age × genotype interaction ($p < 0.01$).

[e]Also significantly different in expression values between *+/sh2* and *sh2/sh2* (genotype effect, $p < 0.01$).

TABLE 4

Genes with a genotype x age interaction, indicating different trends of age-related changes in *+/sh2* vs. *sh2/sh2* mice

Gene symbol	*Gene name*
	RIKEN cDNA B230113M03 gene
Acp1	Acid phosphatase 1, soluble
Akr1c13	Aldo-keto reductase family 1, member C13
Cbx3	Chromobox homolog 3
Cd72	CD72 antigen
Csna	Casein alpha
Cwf19l1	Cwf19-like 1, cell cycle control
Dia1	Diaphanous protein homolog 1
EGF	Epidermal growth factor
Gpsm3	G protein signalling modulator 3
Ihpk1	Inositol hexaphosphate kinase 1
Numa1	Nuclear mitotic apparatus protein 1
P2rx4	Purinergic receptor P2X, ligand-gated ion channel 4[a]
Rbpms	RNA binding protein gene with multiple splicing
Rip3	Rho interacting protein 3
Sparc	Secreted acidic cysteine rich glycoprotein; osteonectin[a]
Tcf3	Transcription factor 3[a]
Tiam1	T cell lymphoma invasion and metastasis 1
Hcngp	Transcriptional regulator protein
Tmem43	transmembrane protein 43
Vdp	Vesicle docking protein
Zfp36l1	Zinc finger protein 36, C3H type-like 1
Zrfp1	Zinc ring finger protein 1

[a]Also showed an overall effect of age, i.e., significant difference in expression values between 3 weeks and 3 months *sh2* mice ($p < 0.01$). Age-related changes in *P2rx4* and *Tcf3* were less than 1.5-fold, thus not listed in this table.

hydroxyapatite contributes to bone ossification (Bolander et al. 1988). Expression of *Sparc* decreased with age in *+/sh2*, *sh2/sh2*, and C57BL/6J mice (Table 3). In addition, its expression, determined by RT-qPCR, was 53% higher in *sh2/sh2* than *+/sh2* mice at 3 weeks ($p < 0.05$), consistent with the age × genotype effect detected in the microarray data. These genes with age × genotype effects might encode proteins involved in cochlear pathology in *sh2/sh2* mice.

DISCUSSION

Gene expression profiling

Analysis of mammalian cDNA libraries derived from human fetal cochlea (Robertson et al. 1994) and from rodent cochlea or organ of Corti (Ryan et al. 1993; Harter et al. 1999; Beisel et al. 2004; Pompeia et al. 2004) has identified likely cochlea-specific genes and proteins important for auditory function. Gene expression profiling with cDNA microarrays further defined the overall pattern of gene expression in the mature cochlea (Cho et al. 2002) and changes in gene expression during cochlear development (Chen and Corey 2002a, b; Hertzano et al. 2004). These approaches contributed substantially to our understanding of pathways critical for development and maintenance of the cochlea and to the identification of genes associated with hearing loss. We now extend these studies to expand our knowledge on molecular events and cellular pathways leading to cochlear pathology.

Gene expression profiling of complex tissues such as the mammalian cochlea presents several challenges, primarily detecting small changes when genes are expressed in only a subset of cells, such as hair cells. For instance, one mouse cochlea is estimated to contain about 3000 hair cells, less than 5% of the entire cell population (Chen and Corey 2002a, b). We demonstrated here, using Affymetrix GeneChips in combination with RMA analysis, that it is possible to reliably detect genes expressed at a wide range of levels, including those expressed in only a limited subset of cell types. We routinely confirmed even small changes in gene expression, such as those observed in *Col15a1* and *Pou2af1*, by RT-qPCR.

Genes with genotype effects

Genes with differential expression in the cochleae of *sh2/sh2* mice might encode proteins that interact directly or indirectly with myosin XV and/or its known interacting proteins. Myosin XV is required to transport whirlin to the tips of stereocilia, probably along actin filaments. Are there other cargos transported by myosin XV? Delprat et al. (2005) proposed that whirlin interacts with a transmembrane protein, NGL-1, isolated from a P2–P6 mouse inner ear cDNA library. In light of similarities between the unconventional myosins XV and VIIa, the PDZ domain proteins whirlin and harmonin, and the transmembrane proteins NGL-1 and cadherin 23, these proteins may form two similar complexes required for stereocilia morphogenesis. These and other interacting proteins are potential candidates that might be affected in the *sh2/sh2* mutants. We found that *Whrn* expression was not affected at the transcriptional level by the *Myo15* mutation in *sh2/sh2* mice at 3 weeks of age (data not shown).

Genes that exhibited differential expression in *sh2/sh2* mice might correspond to proteins involved in cochlear pathology, in altered homeostatic mechanisms, or in compensatory pathways. For example, induction of *Dbi*, which is believed to down-regulate GABA-mediated inhibitory responses, might represent a mechanism to increase neuronal activity in either hair cells or spiral ganglion neurons to compensate for decreased signals from nonfunctional hair cells.

One of the most interesting differentially expressed genes encodes TM4SF3, a member of the superfamily

of membrane proteins containing four transmembrane domains (Maecker et al. 1997). Tetraspanins are known to interact with similar membrane proteins and with integrins at cellular junctions and to assemble small proteins into complex, extensive networks involved in cell–cell signaling. In cancer cell lines, TM4SF3 forms primary complexes with CD9P1 and two other tetraspanins, CD9 and CD81. The primary complexes then interact with yet another tetraspanin CD151, which probably mediates the interaction of the core complex with α3β1 integrin and signaling molecules, such as PI4 kinase and EpCAM (Claas et al. 2005). Mutations in *CD151* cause syndromic sensorineural deafness (Karamatic Crew et al. 2004). These and other tetraspanins may be important in maintaining proper cell–cell interactions and thus crucial for auditory function.

Genes with age-related changes

Genes with age-related changes in mice of both genotypes likely reflect aspects of normal cochlear maturation. The age-related decreases in genes encoding collagens and other ECM proteins are consistent with active remodeling of the ECM in the sensory epithelium or other cochlear structures. We observed decreased expression of genes for collagens types I, III, V, XI, XIII, and XV at 3 months in *sh2/sh2* mutants, as well as in normal-hearing C57BL/6J mice, and BALB/C mice (T.W. Gong, unpublished data), indicating that these decreases are independent of mouse substrain or genotype. An earlier study detected decreased expression of collagen genes in mouse cochlea between postnatal day 2 (P2) and P32 (Chen and Corey 2002a, b). Our findings indicate that down regulation of collagen genes continues beyond 3 weeks of age. Decreased expression of collagen type V may reflect changes occurring either in the tectorial membrane, the otic capsule, or both. In addition, decreases in expression of type I and type XI collagens may represent, at least in part, changes specifically in the sensory epithelium, since these genes are also highly represented in a cDNA library derived from the organ of Corti and adjacent supporting cells (Pompeia et al. 2004). *Sparc* expression is high during embryogenesis and later is primarily restricted to tissues that undergo renewal, remodeling, or repair (for review, see Sage et al. 1989; Schellings et al. 2004). In late embryonic to early postnatal stages of cochlear development, *Sparc* is expressed in the ossifying otic capsule, in stria vascularis, spiral limbus, and spiral ganglion neurons (Mothe and Brown 2001). SPARC is also implicated in cell growth and differentiation via cell–ECM interactions (Yan and Sage 1999).

Two genes in the Wnt/β-catenin signaling pathway, i.e., *Wisp1* and *Tcf3*, were also down-regulated with age. β-Catenin and TCF3/LEF DNA-binding proteins form bipartitate complexes that are translocated to the nucleus to transactivate downstream genes, such as WISP1 (Xu et al. 2000). In the absence of stabilized β-catenin, TCF3 can act as a repressor and plays a critical role in axis formation in the early embryo (Korinek et al. 1998; Merrill et al. 2004). WISP1 plays an important role as an osteoblastic regulator, promoting ostoblast differentiation and chondrocyte proliferation during embryonic skeletal development and repair of fractured bones (French et al. 2004). The lower expression of *Wisp1* in mature cochlea may reflect changes in the otic capsule as well as a potential role as a connective tissue growth factor (see review in Brigstock 2003).

Nephronectin, a component of the basement membrane of several embryonic tissues (Brandenberger et al. 2001), interacts with integrin α8β1 *in vitro* and in embryonic kidney *in vivo* (Brandenberger et al. 2001; Morimura et al. 2001). Mice carrying targeted disruption of *Itga8* for integrin α8β1 have stereocilia defects, suggesting that integrin α8β1 plays a role in regulating hair-cell differentiation and stereocilia maturation (Littlewood Evans and Muller 2000). Early in development (E14.5), nephronectin is found in the basal lamina of the otocyst, but later mainly on the apical epithelial surface outside the developing sensory region (Brandenberger et al. 2001). Integrin α8β1 is found on the apical surface of auditory and vestibular hair cells from E16 to P0 (Littlewood Evans and Muller 2000). Interactions between nephronectin and integrin α8β1 in the sensory epithelium at postnatal stages, particularly at the onset of hearing at 2–3 weeks of age, should be investigated to define the role of these proteins in stereocilia maintenance.

In conclusion, we have demonstrated in this study that Affymetrix microarray analysis, in combination with RMA, is a feasible tool. Previous studies on global gene profiling successfully illustrated how such an approach enables identification of genes that are crucial during ear development and those associated with hereditary deafness (Chen and Corey 2002a, b; Hertzano et al. 2004; Sage et al. 2005). In this study, we extended gene profiling analysis to later stages and showed continuous changes in gene expression beyond 3 weeks of age. These age-related changes in gene expression are likely to reflect the continuing functional maturation of the cochlea, previously observed to reach full maturity at 4 months. At this age, mice also become more resistant to noise-induced hearing loss (Henry 1983). In addition, our analysis of *sh2* mice has uncovered pathways and potential interacting genes that are affected by defective myosin XV. This study marks an essential

initial step in further characterization of these molecules and pathways, not only in *sh2* cochlear pathology but also for proper development and maintenance of auditory function.

ACKNOWLEDGMENTS

This research was supported by the National Institutes of Health through grants R21 DC04920 (MIL), R01s DC09876 (SAC) and DC04410 (DCK), P01 AG025164, in part by the University of Michigan Hearing Research Core Center grant (P30 DC005188) for morphological studies and computational analysis, by a grant from the National Institutes of Digestive and Kidney Disorders (U24 DK58771) to the Michigan Diabetes Research and Training Center for the establishment of the Michigan Biotechnology Core Facility, and by the University of Michigan's Cancer Center Support Grant (5 P30 CA46592). We thank Sarah Davis for assistance with computer analysis and Dr. Donald Swiderski for assistance in assembling SEM photos.

REFERENCES

ANDERSON DW, PROBST FJ, BELYANTSEVA IA, FRIDELL RA, BEYER L, MARTIN DM, WU D, KACHAR B, FRIEDMAN TB, RAPHAEL Y, CAMPER SA. The motor and tail regions of myosin XV are critical for normal structure and function of auditory and vestibular hair cells. Hum. Mol. Genet. 9:1729–1738, 2000.

ANNIKO M, SOBIN A, WERSALL J. Vestibular hair cell pathology in the Shaker-2 mouse. Arch. Otorhinolaryngol. 226:45–50, 1980.

BEISEL KW, SHIRAKI T, MORRIS KA, POMPEIA C, KACHAR B, ARAKAWA T, BONO H, KAWAI J, HAYASHIZAKI Y, CARNINCI P. Identification of unique transcripts from a mouse full-length, subtracted inner ear cDNA library. Genomics 83:1012–1023, 2004.

BELYANTSEVA IA, BOGER ET, FRIEDMAN TB. Myosin XVa localizes to the tips of inner ear sensory cell stereocilia and is essential for staircase formation of the hair bundle. Proc. Natl. Acad. Sci. USA 100:13958–13963, 2003.

BELYANTSEVA IA, BOGER ET, NAZ S, FROLENKOV GI, SELLERS JR, AHMED ZM, GRIFFITH AJ, FRIEDMAN TB. Myosin-XVa is required for tip localization of whirlin and differential elongation of hair-cell stereocilia. Nat. Cell Biol. 7:148–156, 2005.

BEYER LA, ODEH H, PROBST FJ, LAMBERT EH, DOLAN DF, CAMPER SA, KOHRMAN DC, RAPHAEL Y. Hair cells in the inner ear of the pirouette and shaker 2 mutant mice. J. Neurocytol. 29:227–240, 2000.

BOLANDER ME, YOUNG MF, FISHER LW, YAMADA Y, TERMINE JD. Osteonectin cDNA sequence reveals potential binding regions for calcium and hydroxyapatite and shows homologies with both a basement membrane protein (SPARC) and a serine proteinase inhibitor (ovomucoid). Proc. Natl. Acad. Sci. USA 85:2919–2923, 1988.

BRANDENBERGER R, SCHMIDT A, LINTON J, WANG D, BACKUS C, DENDA S, MULLER U, REICHARDT LF. Identification and characterization of a novel extracellular matrix protein nephronectin that is associated with integrin alpha8beta1 in the embryonic kidney. J. Cell Biol. 154:447–458, 2001.

BRIGSTOCK DR. The CCN family: a new stimulus package. J. Endocrinol. 178:169–175, 2003.

CHEN ZY, COREY DP. An inner ear gene expression database. J. Assoc. Res. Otolaryngol. 3:140–148, 2002a.

CHEN ZY, COREY DP. Understanding inner ear development with gene expression profiling. J. Neurobiol. 53:276–285, 2002b.

CHO Y, GONG TW, STOVER T, LOMAX MI, ALTSCHULER RA. Gene expression profiles of the rat cochlea, cochlear nucleus, and inferior colliculus. J. Assoc. Res. Otolaryngol. 3:54–67, 2002.

CLAAS C, WAHL J, ORLICKY DJ, KARADUMAN H, SCHNOLZER M, KEMPF T, ZOLLER M. The tetraspanin D6.1A and its molecular partners on rat carcinoma cells. Biochem. J. 2005.

COSTA E, GUIDOTTI A. Diazepam binding inhibitor (DBI): a peptide with multiple biological actions. Life Sci. 49:325–344, 1991.

DELPRAT B, MICHEL V, GOODYEAR R, YAMASAKI Y, MICHALSKI N, EL-AMRAOUI A, PERFETTINI I, LEGRAIN P, RICHARDSON G, HARDELIN JP, PETIT C. Myosin XVa and whirlin, two deafness gene products required for hair bundle growth, are located at the stereocilia tips and interact directly. Hum. Mol. Genet. 14:401–410, 2005.

DEOL MS. The anatomy and development of the mutants shaker-2, varitint waddler and jerker. J. Genet. 52:562–588, 1954.

DEOL MS. The anatomy and development of the mutants pirouette, shaker-1 and waltzer. Proc. R. Soc. B 145:206–213, 1955.

EISEN MB, SPELLMAN PT, BROWN PO, BOTSTEIN D. Cluster analysis and display of genome-wide expression patterns. Proc. Natl. Acad. Sci. USA 95:14863–14868, 1998.

FRENCH DM, KAUL RJ, D'SOUZA AL, CROWLEY CW, BAO M, FRANTZ GD, FILVAROFF EH, DESNOYERS L. WISP-1 is an osteoblastic regulator expressed during skeletal development and fracture repair. Am. J. Pathol. 165:855–867, 2004.

FRIEDMAN TB, HINNANT JT, GHOSH M, BOGER ET, RIAZUDDIN S, LUPSKI JR, POTOCKI L, WILCOX ER. DFNB3, spectrum of MYO15A recessive mutant alleles and an emerging genotype–phenotype correlation. Adv. Otorhinolaryngol 61:124–130, 2002.

GIORDANO TJ, SHEDDEN KA, SCHWARTZ DR, KUICK R, TAYLOR JM, LEE N, MISEK DE, GREENSON JK, KARDIA SL, BEER DG, RENNERT G, CHO KR, GRUBER SB, FEARON ER, HANASH S. Organ-specific molecular classification of primary lung, colon, and ovarian adenocarcinomas using gene expression profiles. Am. J. Pathol. 159:1231–1238, 2001.

GOPALAKRISHNAN R, OUYANG H, SOMERMAN MJ, MCCAULEY LK, FRANCESCHI RT. Matrix gamma-carboxyglutamic acid protein is a key regulator of PTH-mediated inhibition of mineralization in MC3T3-E1 osteoblast-like cells. Endocrinology 142:4379–4388, 2001.

HALL A. Rho GTPases and the actin cytoskeleton. Science 279:509–514, 1998.

HALL MO, OBIN MS, PRIETO AL, BURGESS BL, ABRAMS TA. Gas6 binding to photoreceptor outer segments requires gamma-carboxyglutamic acid (Gla) and Ca(2+) and is required for OS phagocytosis by RPE cells *in vitro*. Exp. Eye Res. 75:391–400, 2002.

HALL MO, AGNEW BJ, ABRAMS TA, BURGESS BL. The phagocytosis of os is mediated by the PI3-kinase linked tyrosine kinase receptor, mer, and is stimulated by GAS6. Adv. Exp. Med. Biol. 533:331–336, 2003.

HARTER C, RIPOLL C, LENOIR M, HAMEL CP, REBILLARD G. Expression pattern of mammalian cochlea outer hair cell (OHC) mRNA: screening of a rat OHC cDNA library. DNA Cell Biol. 18:1–10, 1999.

HENRY KR. Lifelong susceptibility to acoustic trauma: changing patterns of cochlear damage over the life span of the mouse. Audiology 22:372–383, 1983.

HERTZANO R, MONTCOUQUIOL M, RASHI-ELKELES S, ELKON R, YUCEL R, FRANKEL WN, RECHAVI G, MOROY T, FRIEDMAN TB, KELLEY MW, AVRAHAM KB. Transcription profiling of inner ears from Pou4f3(ddl/ddl) identifies Gfi1 as a target of the Pou4f3 deafness gene. Hum. Mol. Genet. 13:2143–2153, 2004.

HESSLE L, JOHNSON KA, ANDERSON HC, NARISAWA S, SALI A, GODING JW, TERKELTAUB R, MILLAN JL. Tissue-nonspecific alkaline phosphatase and plasma cell membrane glycoprotein-1 are central antagonistic regulators of bone mineralization. Proc. Natl. Acad. Sci. USA 99:9445–9449, 2002.

IRIZARRY RA, BOLSTAD BM, COLLIN F, COPE LM, HOBBS B, SPEED TP. Summaries of Affymetrix GeneChip probe level data. Nucleic Acids Res. 31:e15, 2003.

KARAMATIC CREW V, BURTON N, KAGAN A, GREEN CA, LEVENE C, FLINTER F, BRADY RL, DANIELS G, ANSTEE DJ. CD151, the first member of the tetraspanin (TM4) superfamily detected on erythrocytes, is essential for the correct assembly of human basement membranes in kidney and skin. Blood 104:2217–2223, 2004.

KAROLYI IJ, PROBST FJ, BEYER L, ODEH H, DOOTZ G, CHA KB, MARTIN DM, AVRAHAM KB, KOHRMAN D, DOLAN DF, RAPHAEL Y, CAMPER SA. Myo15 function is distinct from Myo6, Myo7a and pirouette genes in development of cochlear stereocilia. Hum. Mol. Genet. 12:2797–2805, 2003.

KIKKAWA Y, MBURU P, MORSE S, KOMINAMI R, TOWNSEND S, BROWN SD. Mutant analysis reveals whirlin as a dynamic organizer in the growing hair cell stereocilium. Hum. Mol. Genet. 14:391–400, 2005.

KORINEK V, BARKER N, WILLERT K, MOLENAAR M, ROOSE J, WAGENAAR G, MARKMAN M, LAMERS W, DESTREE O, CLEVERS H. Two members of the Tcf family implicated in Wnt/beta-catenin signaling during embryogenesis in the mouse. Mol. Cell Biol. 18:1248–1256, 1998.

LIANG Y, WANG A, BELYANTSEVA IA, ANDERSON DW, PROBST FJ, BARBER TD, MILLER W, TOUCHMAN JW, JIN L, SULLIVAN SL, SELLERS JR, CAMPER SA, LLOYD RV, KACHAR B, FRIEDMAN TB, FRIDELL RA. Characterization of the human and mouse unconventional myosin XV genes responsible for hereditary deafness DFNB3 and shaker 2. Genomics 61:243–258, 1999.

LITTLEWOOD EVANS A, MULLER U. Stereocilia defects in the sensory hair cells of the inner ear in mice deficient in integrin alpha8beta1. Nat. Genet. 24:424–428, 2000.

LIVAK KJ, SCHMITTGEN TD. Analysis of relative gene expression data using real-time quantitative PCR and the 2(-Delta Delta C(T)) method. Methods 25:402–408, 2001.

MAECKER HT, TODD SC, LEVY S. The tetraspanin superfamily: molecular facilitators. FASEB J. 11:428–442, 1997.

MELARAGNO MG, FRIDELL YW, BERK BC. The Gas6/Axl system: a novel regulator of vascular cell function. Trends Cardiovasc. Med. 9:250–253, 1999.

MERMALL V, POST PL, MOOSEKER MS. Unconventional myosins in cell movement, membrane traffic, and signal transduction. Science 279:527–533, 1998.

MERRILL BJ, PASOLLI HA, POLAK L, RENDL M, GARCIA-GARCIA MJ, ANDERSON KV, FUCHS E. Tcf3: a transcriptional regulator of axis induction in the early embryo. Development 131:263–274, 2004.

MORIMURA N, TEZUKA Y, WATANABE N, YASUDA M, MIYATANI S, HOZUMI N, TEZUKA KI K. Molecular cloning of POEM: a novel adhesion molecule that interacts with alpha8beta1 integrin. J. Biol. Chem. 276:42172–42181, 2001.

MOTHE AJ, BROWN IR. Expression of mRNA encoding extracellular matrix glycoproteins SPARC and SC1 is temporally and spatially regulated in the developing cochlea of the rat inner ear. Hear. Res. 155:161–174, 2001.

POMPEIA C, HURLE B, BELYANTSEVA IA, NOBEN-TRAUTH K, BEISEL K, GAO J, BUCHOFF P, WISTOW G, KACHAR B. Gene expression profile of the mouse organ of Corti at the onset of hearing. Genomics 83:1000–1011, 2004.

PROBST FJ, FRIDELL RA, RAPHAEL Y, SAUNDERS TL, WANG A, LIANG Y, MORELL RJ, TOUCHMAN JW, LYONS RH, NOBEN-TRAUTH K, FRIEDMAN TB, CAMPER SA. Correction of deafness in shaker-2 mice by an unconventional myosin in a BAC transgene. Science 280:1444–1447, 1998.

RAJINI B, GRAHAM C, WISTOW G, SHARMA Y. Stability, homodimerization, and calcium-binding properties of a single, variant betagamma-crystallin domain of the protein absent in melanoma 1 (AIM1). Biochemistry 42:4552–4559, 2003.

RAY ME, WISTOW G, SU YA, MELTZER PS, TRENT JM. AIM1, a novel non-lens member of the betagamma-crystallin superfamily, is associated with the control of tumorigenicity in human malignant melanoma. Proc. Natl. Acad. Sci. USA 94:3229–3234, 1997.

RESENDES BL, ROBERTSON NG, SZUSTAKOWSKI JD, RESENDES RJ, WENG Z, MORTON CC. Gene discovery in the auditory system: characterization of additional cochlear-expressed sequences. J. Assoc. Res. Otolaryngol. 3:45–53, 2002.

ROBERTSON NG, KHETARPAL U, GUTIERREZ-ESPELETA GA, BIEBER FR, MORTON CC. Isolation of novel and known genes from a human fetal cochlear cDNA library using subtractive hybridization and differential screening. Genomics 23:42–50, 1994.

RYAN AF, BATCHER S, BRUMM D, O'DRISCOLL K, HARRIS JP. Cloning genes from an inner ear cDNA library. Arch. Otolaryngol. Head Neck Surg. 119:1217–1220, 1993.

SAGE C, HUANG M, KARIMI K, GUTIERREZ G, VOLLRATH MA, ZHANG DS, GARCIA-ANOVEROS J, HINDS PW, CORWIN JT, COREY DP, CHEN ZY. Proliferation of functional hair cells *in vivo* in the absence of the retinoblastoma protein. Science 307:1114–1118, 2005.

SAGE H, VERNON RB, DECKER J, FUNK S, IRUELA-ARISPE ML. Distribution of the calcium-binding protein SPARC in tissues of embryonic and adult mice. J. Histochem. Cytochem. 37:819–829, 1989.

SCHELLINGS MW, PINTO YM, HEYMANS S. Matricellular proteins in the heart: possible role during stress and remodeling. Cardiovasc. Res. 64:24–31, 2004.

SERRU V, LE NAOUR F, BILLARD M, AZORSA DO, LANZA F, BOUCHEIX C, RUBINSTEIN E. Selective tetraspan–integrin complexes (CD81/alpha4beta1, CD151/alpha3beta1, CD151/alpha6beta1) under conditions disrupting tetraspan interactions. Biochem. J. 340 (Pt 1):103–111, 1999.

SKVORAK AB, WENG Z, YEE AJ, ROBERTSON NG, MORTON CC. Human cochlear expressed sequence tags provide insight into cochlear gene expression and identify candidate genes for deafness. Hum. Mol. Gen. 8:439–452, 1999.

SOTIROPOULOS A, GINEITIS D, COPELAND J, TREISMAN R. Signal-regulated activation of serum response factor is mediated by changes in actin dynamics. Cell 98:159–169, 1999.

STOREY JD. A direct approach to false discovery rates. J. R. Stat. Soc., Ser. B 64:479–498, 2002.

TEICHMANN U, RAY ME, ELLISON J, GRAHAM C, WISTOW G, MELTZER PS, TRENT JM, PAVAN WJ. Cloning and tissue expression of the mouse ortholog of AIM1, a betagamma-crystallin superfamily member. Mamm. Genome. 9:715–720, 1998.

WANG A, LIANG Y, FRIDELL RA, PROBST FJ, WILCOX ER, TOUCHMAN JW, MORTON CC, MORELL RJ, NOBEN-TRAUTH K, CAMPER SA, FRIEDMAN TB. Association of unconventional myosin MYO15 mutations with human nonsyndromic deafness DFNB3. Science 280:1447–1451, 1998.

XIANG Z, BO X, BURNSTOCK G. P2X receptor immunoreactivity in the rat cochlea, vestibular ganglion and cochlear nucleus. Hear. Res. 128:190–196, 1999.

XU L, CORCORAN RB, WELSH JW, PENNICA D, LEVINE AJ. WISP-1 is a Wnt-1- and beta-catenin-responsive oncogene. Genes Dev. 14:585–595, 2000.

YAN Q, SAGE EH. SPARC, a matricellular glycoprotein with important biological functions. J. Histochem. Cytochem. 47:1495–1506, 1999.

YANAGITA M. The role of the vitamin K-dependent growth factor Gas6 in glomerular pathophysiology. Curr. Opin. Nephrol. Hypertens. 13:465–470, 2004.